WISCONSIN
INDIANA
YALE
NOAO

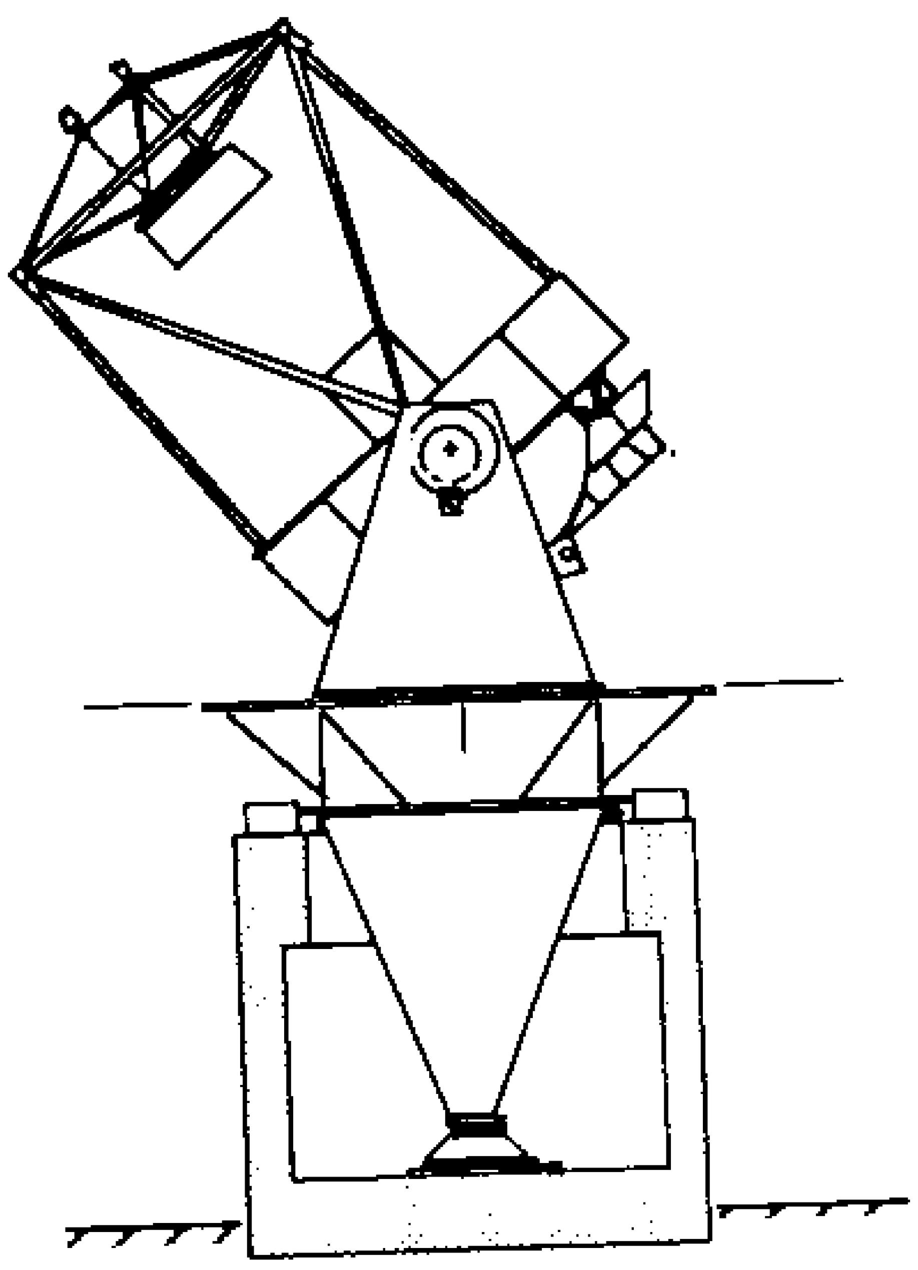

3.5 METER TELESCOPE

Optical Design, Tolerances & Alignment for the WIYN 3.5 Meter Telescope

No. WODC 02-01-01

Draft

4/12/91

1. Purpose and Scope

2. Optical Design

In this section we present the optical design of the telescope and an analysis of the degradation of image quality due to misalignment of the optics.

A major project requirement is for an optical design optimized for multi-object, fiberoptic spectroscopy. A 1° field of view is specified to insure there will be an adequate number of objects in the field for the number of fibers and types of programs contemplated. The focal ratio will be selected to minimize the effects of focal ratio degradation and at the same time provide adequate beam scrambling in the fiber to improve the precision of radial velocity measurements. Finally, a telecentric design is preferred to simplify the design of the fiber input and reduce losses around the spectrograph collimator.

A second project requirement is that there be a narrower field optimized to produce sharp images for use by CCDs and other university instruments. The field of view for these applications needs to be wide enough to cover the largest foreseeable single CCDs without the need for refractive correcting elements in the beam. The plate scale should be such that good images are adequately, but not over, sampled.

The two Nasmyth foci are used to satisfy these requirements. One port, the MOS port, is optimized for wide field applications and has a wide field corrector permanently mounted in the instrument rotator. The other port, the WIN port, is used for all other applications.

The uncorrected field of view of the classical Cassegrain design is clearly inadequate for even the narrow field applications. A Ritchey-Chrétien design is specified.

2.1 Focal ratio

The selection of final focal ratio for the telescope was driven by the requirement that the telescope couple efficiently to the 200 micron optical fibers of the MOS. Barden[1] has shown that focal ratio degradation becomes a problem with optical fibers for focal ratios slower than about f/7. The problem manifests itself as inefficient coupling to the spectrograph being fed by the fibers. He has also shown that the radial scrambling of the beam in the fibers required for radial velocity measurements and velocity dispersions is less complete for focal ratios faster than about f/5.5.[2] These two characteristics of the fibers bracket the optimal focal ratio for the telescope.

[1] S. Barden,

[2] S. Barden, Private communication, 1989.

The faster focal ratios have the additional penalty that the size and weight of the secondary mirror becomes greater increasing both the degree of central obscuration and the difficulty of rigidly supporting the mirror.

Considering these issues, a focal ratio of f/6.3 was selected as optimal for the MOS applications. This gives a telescope focal length of 22.0 meters and a plate scale of 9.36 arcsec./mm..

(Brodie's results of transmission through an aperture.)

A requirement for the WIYN port is that the images produced during times of good seeing should be adequately sampled by CCDs. The image error budget for the narrow field port specifies that the image degradation due to the telescope and dome will not not exceed 0.40 arcsec. FWHM. This will degrade 0.7 arcsec. seeing to about 0.8 arcsec. Approximately three pixels across this diameter will be necessary to adequately sample the image and still be able to take advantage of periods of better seeing.

While it is not certain what size pixels will be available at the time the WIYN telescope is completed, the trend is towards pixels smaller than the 30 mm pixels of the Tektronix 2048s. 23 μm, or even 15 μm, pixels are more likely to be common.

A 0.8 arcsec. image has a diameter of 86 mm at f/6.3. While this is near optimal for the Tektronix CCDs, it may be slightly oversampled by the smaller pixels. Nevertheless, having to provide only a single focal ratio for both ports is a major advantage and f/6.3 is adopted for the WIYN port as well.

2.2 Basic Ritchey-Chrétien design

Primary mirror:

Diameter	D_1	3.5	meters
Focal ratio	F_1	1.75	
Focal length	f_1	6.1250	meters
Conic constant	K_1	-1.070833	

Secondary mirror:

Full Diameter		1.200	meters
Clear diameter	D_2	1.173	meters
Focal length	f_2	-2.6611	meters
Conic constant	K_2	-3.731667	

Tertiary mirror:

Major clear diameter	1.058	meters
Minor clear diameter	0.748	meters
Major full diameter	1.100	meters
Minor full diameter	0.800	meters
Radius of curvature	∞ (Plane)	

System parameters:

Focal ratio	F	6.295	
Focal length	f	22.0341	meters
Angular Field of view radius	Θ	8.727×10^{-3}	radians
Field of view, diameter		1.0	degree
Magnification	m	3.597	
Primary-secondary separation	d	4.2000	meters
Back focal distance	e	2.7270	meters
Plate scale		9.36	arcsec./mm
Reciprocal plate scale		0.107	mm/arcsec.
Linear field size, 15 arcmin.		96	mm
Linear field size, 1°		385	mm
Field curvature, Bare R-C		2.114	meters
Field curvature w/W-F corrector		5.510	meters

2.3 Image quality

3. Wide field corrector

3.1 WF Corrector Prescription

3.2 Wide-field Image quality

4. ADC/corrector

4.1 ADC Prescription

4.2 ADC Image quality

5. Optical surface and support specifications

The strategy that is becoming common in specifying the quality of the optical surfaces in a telescope is to specify the maximum permitted phase errors as a function of separation between measuring points with a structure function similar to that which describes the wavefront errors produced by the atmosphere. The structure functions depend on the spatial separation of measurement points and have the property that the specification is not too stringent for low spatial frequencies nor too loose for high ones as might be the case when a single number is used to specify surface quality. The advantage of this approach is that the optical system can be specified such that the contribution due to the optics is always less than the atmospheric contribution. This method was first used by D. Brown[1] at Grubb-Parsons to polish the 4.2 m William Herschel Telescope.

Turbulence in the atmosphere produces phase shifts in the wavefront from a distant object that vary across the aperture of the telescope. The rms phase error between any two points on the wavefront is a function of their separation and may be described by the Kolmogorov scaling law, which, expressed as a linear difference, yields the rms difference equation:

$$\delta(x) = 0.42\,\lambda \left(\frac{x}{r_0}\right)^{5/6} \qquad (5.1)$$

[1] D. Brown, "Optical Specification of Ground Based Telescopes", Proc. SPIE 399, 1983.

x = Separation between measurement points,
λ = Wavelength,
r_0 = Fried's parameter, a measure of seeing that grows as $\lambda^{1.2}$.

When r_0 is less than the telescope aperture, D, the seeing disk is given by Martin[1] :

$$\Delta\ (\mathrm{FWHM}) = 0.98\ \left(\frac{\lambda}{r_0}\right) \tag{5.2}$$

Δ is often specified for the standard wavelength 500 nm. r_0(500 nm) is 14.4 cm for 0.7 arcsecond seeing FWHM.

Eq. 2.1 may be used to specify mirror surface quality by chosing an appropriate value of r_0 from the image error budget. At small spatial scales ($d \ll r_0$) the specification obtained from eq. 2.1 may be relaxed. At these scales, the effect of surface roughness is to scatter light out of the diffraction core of the image. Ruze[2] gives the fractional loss as:

$$\Gamma = \left(\frac{2\pi\sigma}{\lambda}\right)^2 \tag{5.3}$$

where σ is the rms deviation from the mean wavefront. The maximum permitted loss due to scattering determines the high spatial frequency surface specification.

Tilt in the wavefront produces pointing errors in the image plane. Since these are included elsewhere in the image error budget, they should be removed from the optical surface specification. Martin[op. cit.] shows that the effect of removing tilt is to roll the structure function off at separations comparable to the aperture of the mirror. The modified structure function including allowance for scattering and tilt becomes:

$$\delta^2(x) = 2\sigma^2 + 0.17\ \lambda^2\ \left(\frac{x}{r_0}\right)^{5/3}\ \left(1 - 0.975\ \left(\frac{x}{D}\right)^{1/3}\right) \tag{5.4}$$

where D is the aperture of the mirror.

The allowed rms departure of the mirror surface from the desired figure is half of the rms wavefront difference. The peak-to-value surface tolerance is approximately 4 times the rms tolerance.

5.1 Primary mirror

The error budget for the primary mirror is 0.2 arcseconds FWHM which corresponds to r_0= 51 cm at 500 nm. The contributions to the primary error budget are:

	FWHM (arcsec)	r_0(500 nm)	Scattering(500 nm)
Figuring	0.09	112	0.03

[1] H. M Martin, "Image Motion as a Measure of Seeing Quality", PASP **99**, pg. 1360,1987.

[2] J. Ruze, "Antenna Tolerance Theory-A Review", Proc. IEEE **54**, no. 4, 1966.

Thermal	0.16	63	0.00
Supports	0.09	112	0.00

Figure 2.xxx shows the structure functions for polishing and supporting the primary mirror. The desired surface specification is given by:

Separation (cm)	dz_{rms} (nm)
2	10
22	23
≥220	75

where dz is the departure of the surface from the desired figure.

5.2 Secondary mirror

The error budget for the secondary mirror is 0.10 arcseconds FWHM which corresponds to r_0(500 nm)= 101 cm at the entrance aperture of the telescope. The effective value for r_0 at the location of the secondary is given by

$$r_{eff} = r_0 \left(\frac{s}{f}\right) \tag{5.5}$$

where s= 6.9 m is the distance from the secondary to the focal plane and f= 22.1 m is the telescope focal length. r_{eff}(500 nm) = 32 cm. The contributions to the secondary error budget are:

	FWHM (arcsec)	r_{eff}(500 nm)	Scattering(500 nm)
Figuring	0.05	63	0.03
Thermal	0.07	45	0.00
Supports	0.05	63	0.00

Figure 2.xxx shows the structure functions for polishing and supporting the secondary mirror. The desired surface specification is given by:

Separation (cm)	dz_{rms} (nm)
(smoothness) ≤2	11
6.6	16
25	33
≥74	50

where dz is the departure of the surface from the desired figure.

5.3 Tertiary mirror

The error budget for the tertiary mirror is 0.08 arcseconds FWHM which corresponds to r_0(500 nm)= 126 cm at the entrance aperture of the telescope. The mirror is 3.2 m from the focal plane so r_{eff}(500 nm) = 18 cm. The contributions to the tertiary error budget are:

	FWHM (arcsec)	r_{eff}(500 nm)	Scattering(500 nm)
Figuring	0.04	36	0.02
Thermal	0.06	24	0.00

Supports	0.04	36	0.00

Figure 2.xxx shows the structure functions for polishing and supporting the tertiary mirror. The desired surface specification is given by:

Separation (cm)	dz_{rms} (nm)
2	11
10	28
≥60	74

where dz is the departure of the surface from the desired figure.

5.4 Correctors

6. Optical alignment

The fast optical design and highly aspheric secondary mirror described in section 2.1 will require tight positional tolerances of the optical elements to meet the imaging specification. This in turn will require a stiff telescope mount and a control system with some provision for active optical alignment. In this section we look at the effects of misalignment of the telescope optics.

We define the primary axis of the telescope as coincident with the optical axis of the primary mirror with its origin at the vertex of the primary mirror. Tilts and translations of the secondary and tertiary mirrors are relative to the primary axis. The elevation axis is defined by the center of rotation of the elevation bearings and is the reference for the corrector position. In a perfectly aligned telescope with no manufacturing errors the primary and elevation axes would intersect in the center of the optical support structure and would be perpendicular.

Piston is a change of separation between optical elements in the initially focussed telescope. Decentration is a lateral translation of an element with respect to the reference axis. Despace is the difference between the 'as-built' design and actual element spacings. Tilt measures the angle between the reference axis and the optical axis of an element.

6.1 Secondary alignment

Formulas for the optical aberrations in a misaligned two mirror Ritchey-Chrétien system may be found in Faber[1] and Schroeder[2]. Except as noted, the presence of a corrector in the WIYN optical design will not significantly change the aberrations calculated neglecting the corrector.

6.1.1 Focus

Piston of the secondary mirror produces a focus error at the detector. The angular diameter of the blur circle is given by:

---

[1] S. Faber, TMT Technical report No. 55, 1981.

[2] D. Schroeder, "Astronomical Optics", Academic Press, 1987.

$$f = \left(1 + m^2\right) \frac{\delta d}{f\ F} \qquad \text{(Focus)} \qquad (6.1)$$

where δd is the piston and the definitions and values for m, f, and F are given in section 2.1. The conversion to FWHM determined from ray tracing is approximately $\phi_{fwhm} = 0.86\ \phi$. Substituting values and converting to arcseconds we obtain:

$$\frac{\phi_{fwhm}}{\delta d} = 18 \text{ arcsec./mm.} \qquad (6.2)$$

6.1.2 Despace

Despacing of the primary and secondary mirrors produces spherical aberration in the image. The amount of spherical aberration is less than the blur caused by defocus near the nominal focal surface but can be a problem if the back focus of the telescope is changed and the secondary is refocussed to compensate. This could occur as a result of manufacturing errors in the optics or in an instrument that places its focal plane at some position other than the nominal focus. The spherical aberration caused by despace is given by:

$$\frac{\phi}{\delta d} = \frac{m\ (m^2-1)}{16\ f_1\ F^3} \left(1 + \frac{2}{(m-1)\ (m-\Delta)}\right) \quad \text{(Despace SA)} \quad (6.3)$$

From ray tracing we get the empirical relation that $\phi_{fwhm} = 0.33\ \phi$. Substituting values into 2.8 gives:

$$\frac{\phi_{fwhm}}{\delta d} = 0.15 \text{ arcsec./mm} \qquad \text{(Despace SA)} \qquad (6.4)$$

If the telescope is focussed at a position different from the optimal focus, the spherical aberration is given by:

$$\frac{\phi_{fwhm}}{\delta e} = (m^2+1)^{-1} \frac{\phi_{fwhm}}{\delta d} = 1.1 \times 10^{-2} \text{ arcsec./mm} \qquad (6.5)$$

where δe is the distance from the optimal focus.

6.1.3 Tilt and decenter

The principal aberrations produced by decenter and tilt of the secondary are coma and wavefront tilt (ie. pointing errors). Coma produced by decenter can be compensated by an appropriate tilt of the secondary and the same is true for pointing errors although, for a Ritchey-Chrétien, the two can't be compensated simultaneously. The coma is given by:

$$\phi = \frac{-3}{32} \left(\frac{m-1}{F}\right)^3 \frac{\delta x}{D_1} \left(K_2 - \left(\frac{m+1}{m-1}\right)\right) \qquad \text{(Decenter)} \qquad (6.6)$$

$$\phi = \frac{-3\ (1+(e/f_1))\ (m-1)}{16\ F^2}\ \delta e \qquad \text{(Tilt)} \qquad (6.7)$$

where δx and δe are the decenter and tilt respectively. ϕ must be multiplied by approximately 0.50 to get FWHM values. Substituting values for the WIYN optical design:

$$\frac{\phi_{fwhm}}{\delta x} = 1.1 \text{ arcsec/mm} \qquad \text{(Decenter)} \quad (6.8)$$

$$\frac{\phi_{fwhm}}{\delta e} = -8.8 \times 10^{-3} \qquad \text{(Tilt)} \quad (6.9)$$

Setting 2.11 equal to minus 2.12 allows us to solve for δx as a function of δe. This gives us the distance, R, from the secondary vertex to the neutral point on the primary axis about which the secondary may be rotated and produce no coma:

$$R = \frac{\delta x}{\delta e} = 1.7 \text{ m} \qquad (6.10)$$

The neutral point is located above the secondary when the telescope is pointed at the zenith. From section 2.1.2 the center of curvature of the secondary about which the mirror can rotate with zero wavefront tilt (pointing error) is located above the neutral point, 2.66 m above the secondary mirror vertex.

Eventually off-axis astigmatism becomes the limiting factor in how well decenter can be compensated by tilting the secondary. For the bare R-C, a decentration of 0.50 mm produces a 2D rms diameter contribution of 0.1 arcsecond of astigmatism at a field radius of 7.5 arcminute when the tilt and decentration are adjusted to give zero coma at the center of the field.[1] With the wide-field corrector, a decentration of 0.50 mm produces a 2D rms diameter contribution of 0.26 arcseconds of astigmatism at a 21 arcminute field radius.

6.2 Tertiary alignment

6.3 Motion of the primary axis

6.4 Corrector alignment

6.4.1 Corrector Piston

The effects of translating the wide field corrector along the optical axis can be seen in the following table obtained by ray tracing:

Image size (μm)

Piston (mm)	ϕ_{63}max	ϕ_{63}rms	ϕ_{80}max	ϕ_{80}rms
-5.0	23	22	32	30
0.0	17	13	24	18
5.0	14	12	16	15
10.0	30	21	36	25

where $\phi_{63(80)}$ are the diameters for 63% (80%) enclosed energy given both as rms and maximum values. Rays were traced for field angles of 0.0, 0.35°, and 0.5° and given weights of 1, 4, and 4 respectively. Because the rays

[1] M. Johns, "Positioning of the Secondary", WIN Report 4/10/89.

were traced for the single wavelength 500 nm., the optimal position found for the corrector does not necessarily occur at the nominal position.

6.4.2 Decenter

The wide field corrector produces a 0.62% pincushion distortion in the focal plane of the telescope. If the corrector translates perpendicular to the optical axis, there will be a relative shift in the positions of images across the field. At a field radius of 0.5°, the local plate scale is about 1.8% less than at the center of the field. The relative angular displacement, dq, of an image at the edge of the field relative to the center due to a lateral displacement, dx, of the corrector and plate scale 6.288 arcsec/mm is given by:

$$\left(\frac{\delta q}{\delta x}\right)_{\theta=0.5^\circ} = 0.17 \text{ arcsec/mm.} \qquad (6.11)$$

If this occurs during a integration, the error will add arithmetically to the image size.

A lateral translation of the corrector will also affect the image quality. Some parts of the field will degrade while others will actually improve. From ray traces of a number of field angles with the corrector decentered 1 mm., the worst case contribution to image blur was found to be ϕ = 0.17 arcsec. at a field angle of θ = 0.35°.

6.4.3 Tilt

The effects of tilting the corrector can be seen in the following table obtained by ray tracing (λ = 500 nm). Nine pencils of rays were traced at field angles of 0°, 0.35° (4 rays) and 0.5° (4 rays) for each case .

	Image size (μm)				Field distortion (μm)	
Tilt (arcmin)	ϕ_{63}max	ϕ_{63}rms	ϕ_{80}max	ϕ_{80}rms	θ = 0.35°	θ = 0.5°
0.0	17	13	24	18	0	0
1.0	19	13	26	18	1	2.5
10.0	29	17	39	19	10	27

where ϕ63(80) are the diameters for 63% (80%) enclosed energy given both as rms and maximum values sampled at nine positions in the field.

6.5 Summary

D.B.

STRUCTURE FUNCTION FOR Ro = 112.2998 (9.000001E-02 FWHM) 02-04-1991
TILT HAS BEEN REMOVED
.5 % SCATTER HAS BEEN ADDED
WAVELENGTH IS 500 NM

X (CM)	RMS WAVEFRONT ERROR (NM)
.5	5
1	6
2	8
5	14
6.6	17
10	23
20	39
25	46
30	52
50	74
74	95
350	85

STRUCTURE FUNCTION FOR Ro = 202.1397 (.05 FWHM) 02-04-1991
SPATIAL SCALING 120 : 350
TILT HAS BEEN REMOVED
.5 % SCATTER HAS BEEN ADDED
WAVELENGTH IS 500 NM

X (CM)	RMS WAVEFRONT ERROR (NM)
.5	6
1	7
2	10
5	19
6.6	23
10	31
20	50
25	58
30	64
50	83
74	91
120	52

STRUCTURE FUNCTION FOR Ro = 252.6746 (.04 FWHM) 02-04-1991
SPATIAL SCALING 50.5 : 350
TILT HAS BEEN REMOVED
.1 % SCATTER HAS BEEN ADDED
WAVELENGTH IS 500 NM

X (CM)	RMS WAVEFRONT ERROR (NM)
.5	5
1	9
2	15
5	29
6.6	35
10	46
20	67
25	72
30	75
50	45